Conformational Analysis of γ' Peptide (410−427) Interactions with Thrombin Anion Binding Exosite II†

T. Michael Sabo,‡ David H. Farrell,§ and Muriel C. Maurer*,‡

Department of Chemistry, University of Louisville, 2320 South Brook Street, Louisville, Kentucky 40292, and Department of Pathology, School of Medicine, Oregon Health and Science University, Portland, Oregon 97239-3098

Received February 21, 2006; Revised Manuscript Received April 19, 2006

ABSTRACT: Thrombin utilizes two anion binding exosites to supplement binding of fibrinogen to this serine protease. Approximately 7−15% of the fibrinogen γ chain exists as the highly anionic γ' variant (^{408}-VRPEHPAETEY$_S$DSLY$_S$PEDDL^{427}). This segment has been demonstrated to target thrombin ABE-II and can accommodate sites of phosphorylation in place of sulfonation without sacrificing binding affinity. The present work employed 1D and 2D solution NMR to characterize the structural features of the bound γ' peptide (410−427) and to evaluate the requirement of sulfonation for effective thrombin interaction. The results indicate the γ' residues 414−427 make significant contact with the enzyme, a β-turn exists between residues 422−425 in the presence of thrombin, and there is a large cluster of through-space interactions involving residues 418−422. Effective contact with ABE-II requires the presence of at least one phosphotyrosine residue with Y$_P^{422}$ being the more important player. Hydrogen−deuterium exchange (HDX) coupled with MALDI-TOF MS was implemented to examine the location of the γ' peptide−thrombin interface and to screen for changes in solvent exposure at distant sites. The HDX results demonstrate that the γ' peptide interacts with or is in close proximity to thrombin residues R^{93}, R^{97}, R^{173}, and R^{175}. The binding of the γ' peptide also protects other regions of thrombin from deuterium exchange. Affected regions include segments of ABE-I, the autolysis loop, the edge of the active site region, and the A-chain. Finally, thrombin forms a ternary complex with the γ' peptide and PPACK, generating an enzyme whose solvent-exposed regions are even further stabilized from HDX.

The serine protease thrombin possesses the ability to promote both procoagulant and anticoagulant events (*1*, *2*). Interactions with substrates and ligands all contribute to balancing the multifaceted activity of thrombin. Substrates for thrombin include fibrinogen, factor V, factor VIII, factor XI, factor XIII, protein C, and the protease-activated receptors PAR1 and PAR4. Thrombin contains two exosites that are located on opposing faces of the serine protease flanking the catalytic site (*3*) (Figure 1). These highly electropositive patches are termed anion binding exosites I and II (ABE-I and ABE-II).[1]

As with ABE-I, a variety of ligands target ABE-II, resulting in different physiological consequences. Heparin participates in a ternary complex with thrombin ABE-II and the serpin antithrombin III that leads to the inactivation of thrombin (*5*). FVIII binds to ABE-II, aiding in thrombin cleavage of the FVIII residues R^{372}-S^{373} and, as a result, amplifies coagulation (*6*). On the surface of platelets, the association of GpIbα with ABE-II accelerates thrombin activation of PAR1, while reducing the rate of fibrinopeptide A release from fibrin (*7*, *8*). A recent crystal structure of haemadin and thrombin demonstrates the necessity of both ABE-II and the active site for this inhibitory interaction (*9*). Finally, a C-terminal variant of the fibrinogen γ chain has been demonstrated to bind to ABE-II (*10*, *11*).

Fibrinogen (AαB$\beta\gamma_A$)$_2$ is a dimer comprised of three domains existing as coiled coils in the shape of a dumbbell (*12*, *13*). The N-termini of all six polypeptide chains are located in the center E-domain of fibrinogen. This region supplies a low-affinity binding site for thrombin via ABE-I (*14*). The C-termini of the polypeptide chains reach laterally from the E-domain to form the flanking D-domains. There are two variants of the γ chain carboxy terminus extending outward from the D-domains (*15*, *16*). The γ_A chain terminates with four amino acids (^{408}AGDV^{411}). The C-terminus of the γ_A chain interacts with platelets through residues 400−411 (*17*). The γ' chain results from a mRNA splice variant due to alternative processing and replaces the last four residues of the γ_A chain with an insertion of 20 amino acids (^{408}VRPEHPAETEYDSLYPEDDL^{427}) (*18*, *19*). About 7−15% of all fibrinogen exists as the γ_A/γ' heterodimer as opposed to the more common γ_A/γ_A homodimer (*20*, *21*).

† Funding for this project was supported by NIH Grants R01 HL68440 (to M.C.M.) and R21 HL75006 (to D.H.F.).

* To whom correspondence should be addressed. Tel: 502-852-7008. Fax: 502-852-8149. E-mail: muriel.maurer@louisville.edu.

‡ University of Louisville.

§ Oregon Health and Science University.

[1] Abbreviations: FV, FVIII, FXI, and FXIII, blood clotting factors V, VIII, XI, and XIII; IIa, thrombin; ABE-I, anion binding exosite I; ABE-II, anion binding exosite II; PAR1, protease-activated receptor 1; K_D, equilibrium binding constant; GpIbα, glycoprotein Ibα; Fbg, fibrinogen; PPACK, D-Phe-Pro-Arg chloromethyl ketone; Y$_S$, sulfotyrosine; Y$_P$, phosphotyrosine; TCEP, tris(2-carboxyethyl)phosphine hydrochloride; NMR, nuclear magnetic resonance; 1D, one dimensional; 2D, two dimensional; TOCSY, total correlation spectroscopy; tr-NOESY, transferred nuclear Overhauser effect spectroscopy; MALDI-TOF MS, matrix-assisted laser desorption−ionization time-of-flight mass spectrometry; HDX, hydrogen−deuterium exchange.

10.1021/bi060360k CCC: $33.50
Published on Web 05/23/2006

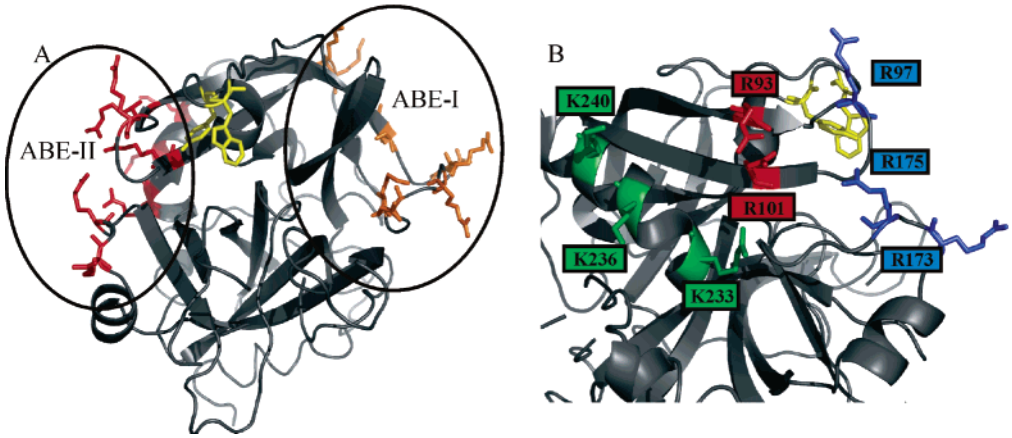

FIGURE 1: The anion binding exosites of thrombin (1PPB). (A) Location of the two anion binding exosites in relation to Y^{60A} and W^{60D} (yellow residues). ABE-I is represented by orange residues, and ABE-II is represented by red residues. (B) ABE-II presented in more detail. The cationic residues are placed into three groups: central ABE-II binding hot spot (red), C-terminal region (green), and residues near the substrate specificity pockets (blue). These figures were created using PyMol (*4*).

Table 1: Sequences of Selected ABE-II Binding Sites[a,b]

fibrinogen γ′	^{408}VRP**E**HPA**ET**E**Y$_S$**D**SL**Y$_S$**P**EDD**L^{427}
GpIbα	^{271}G**DT**D**L**Y$_S$**D**Y$_S$**Y$_S$**P**EE^{282}
FVIII	^{341}**EEA**E**DY$_S$DDD**LT**D**SE**M^{355}

[a] Anionic residues are in bold. [b] These human ABE-II binding sequences were taken from the following sources: fibrinogen γ′ (*25*, *26*), GpIbα (*27*), and factor VIII (*28*).

Sulfonation appears to be an important element in directing ligand binding to thrombin. In 1954, Bettelheim first reported the presence of sulfonation in a blood coagulant protein at Y^6 of the bovine fibrinogen Bβ chain (*22*). This modified residue probably aids in interaction of the Bβ chain with the extended active site region and, possibly, ABE-II. Other well-known sulfonated ligands are the ABE-I binding active site inhibitor hirudin (*23*) and the ABE-II targeting heparin sulfate (*24*). The ABE-II binding sequences of the γ′ peptide (*25*, *26*), GpIbα (*27*), and FVIII (*28*) all display a similar intense clustering of sulfotyrosine, aspartate, and glutamate residues (Table 1). Within the γ′ peptide, there are two sulfonated tyrosine residues along with seven aspartate and glutamate amino acids. Replacement of the sulfotyrosines with phenylalanines in the γ′ region of fibrin abolishes ABE-II binding (*10*).

Meh et al. demonstrated that the D-domain region of fibrinogen γ_A/γ' contained a high-affinity binding site for thrombin with a K_D of 0.26 μM (*29*). Further work implicated the γ′ residues A^{414}−L^{427} as essential to the high-affinity interaction, although the exact location of the γ′ chain interface on thrombin was unclear (*25*). Subsequent competitive fluorescent binding studies localized γ′ peptide binding to ABE-II with a K_D in the 0.63−2.2 μM range for residues V^{408}−L^{427} (*10*, *11*). A combination of heparin, hirudin fragments, and DNA aptamers targeting ABE-I and -II were employed to verify the site of interaction (*10*, *11*). The γ′ chain of fibrinogen has also been demonstrated to be a carrier of plasma factor XIII (A_2B_2) via the FXIII B_2 subunits (*30*). The presence of elevated levels of the heterodimer γ_A/γ' has been linked to increased incidence of cardiovascular diseases. This effect is attributed in part to formation of a clot that is less susceptible to fibrinolysis (*21*).

A crystal structure illustrating γ′ peptide binding to thrombin has not been reported at the present time. As a result, the structure the peptide adopts upon binding to thrombin and the exact ligand interface on the surface of thrombin are unknown. Additionally, a method to observe the regions of thrombin influenced by ligand would help to elucidate how allosteric changes are transmitted from ABE-II through the protease. Phosphotyrosines, which do not sacrifice binding affinity, were prepared instead of the acid-labile sulfotyrosines (*10*, *31*).

One-dimensional and two-dimensional NMR experiments were carried out to observe, in solution, the structural features the γ′ peptide adopts upon interacting with thrombin's ABE-II. Furthermore, the individual residues within the γ′ peptide that contact the enzyme's surface could be detected. In another series of studies, hydrogen/deuterium exchange (HDX) monitored by matrix-assisted laser desorption−ionization time-of-flight mass spectrometry (MALDI-TOF MS) was used to characterize the effects of γ′ peptide binding on the solvent accessibility of thrombin's surface. Additional coverage of thrombin was obtained through the use of the reducing agent TCEP, which enabled the monitoring of previously unseen regions of thrombin.

Our findings describe the γ′ peptide−thrombin relationship from the perspective of both the peptide and the enzyme. γ′ peptide binding to ABE-II causes the ligand to adopt significant secondary structure when compared to free peptide in solution. Interactions at ABE-II also have allosteric consequences on the rate of deuterium exchange for regions unaffiliated with the ligand−protease interface. Specifically, 1D proton line broadening results indicate that residues H^{412}−L^{427} of the γ′ peptide (410−427, $Y_P^{418}Y_P^{422}$) are responsible for the primary sites of contact with the thrombin surface and Y_P^{422} is the dominant player. Two-dimensional tr-NOESY spectra illustrate the importance of a β-turn between residues Y^{422}−D^{425} in the thrombin-bound peptide structure. HDX results localize the γ′ peptide binding surface to residues at or near the thrombin[2] ABE-II amino acids R^{93}, R^{97}, R^{173}, and R^{175}. γ′ peptide binding also affects the deuterium exchange dynamics for distant sites, establishing potential lines of communication from ABE-II to ABE-I, regions near the active site, and a portion of the A-chain.

[2] Throughout the paper, thrombin residues have been referenced according to the chymotrypsin numbering scheme.

MATERIALS AND METHODS

Synthetic Peptides. Peptides based on residues 410−427 (PEHPAETEYDSLYPEDDL) of the human fibrinogen γ' chain were synthesized by SynPep (Dublin, CA) and Research Genetics, Inc. (Huntsville, AL). Four variants of this sequence were prepared: (1) $Y_P^{418}Y_P^{422}$, (2) Y_P^{418}, (3) Y_P^{422}, and (4) an unphosphorylated peptide (Table 2). MALDI-TOF measurements on an Applied Biosystems Voyager DE-Pro mass spectrometer were used to verify the peptide *m*/*z* values. The concentrations of the peptides in solution were determined by quantitative amino acid analysis (AAA Service Laboratory, Inc., Boring, OR).

Thrombin Preparation. The isolation and purification of bovine thrombin from bovine plasma barium sulfate eluate (BSE) (Sigma) were performed as previously described by Trumbo and Maurer (*32*). The purified thrombin solution was concentrated with Amicon Ultra-15 centrifugal filter units (Millipore) in an Allegra 21R centrifuge (Beckman Coulter) run at 4000 rpm and 4 °C. The concentration of the activated thrombin was determined using the extinction coefficient of $E^{1\%} = 19.5$ (*33*); then the activated thrombin was aliquoted and frozen at −70 °C for future use.

Bovine thrombin was used as the enzyme during the course of this work, while peptides derived from the fibrinogen γ' chain were based on the human sequence. Human and bovine thrombins exhibit a high degree of sequence conservation (*3*). Important regions where there are no differences include the active site, the allosteric Na^+ binding site, the thrombin β-insertion (Trp^{60D}) loop, ABE-I, and ABE-II. The interaction of the γ' peptide derived from the human sequence with bovine thrombin is not anticipated to be affected by the minor differences between the species.

Basis for 1D Proton Line Broadening and 2D tr-NOESY NMR Experiments. One-dimensional proton line broadening and two-dimensional transferred nuclear Overhauser effect (tr-NOESY) experiments (*34*, *35*) were performed to probe the conformational and structural characteristics adopted by the γ' peptide upon interacting with thrombin's ABE-II. Peptides with less than 20 amino acids lack significant secondary structure and tumble rapidly when free in solution. Without the presence of the interacting protein, $\omega\tau_c$ approaches 1. This condition yields few NOEs in the transferred NOESY spectrum, while producing a 1D spectrum with well-defined peaks. Upon interacting with the surface of an enzyme, this same peptide now adopts a conformation with distinct secondary structural features. The peptide−enzyme complex increases the $\omega\tau_c$ which promotes the formation of large, negative NOEs that describe the bound state of the peptide. To obtain information about this bound state, the peptide concentration is in molar excess to the enzyme, and the k_{off} has to be sufficiently fast to allow the peptides with secondary structural information to rejoin the free peptides in solution. Since the NOEs relating to the bound structure of the peptide are much larger than the NOEs for the free peptide, information relating to the bound structure of the peptide will dominate the NOESY spectrum. The transverse relaxation time (T_2) is inversely proportional to $\omega\tau_c$, as well as being related to the line width shape of the resonance. Protons that interact with the enzyme surface experience an increase in $\omega\tau_c$, leading to a decrease in T_2. The net effect is line broadening in the 1D spectrum. Differences in line width and/or line shape reflect the contributions of peptide in the bound state transferred to the free population (*34*, *35*).

Table 2: Fibrinogen γ' Peptides Used in the Present Study

$\mathbf{Y_P}^{418}\mathbf{Y_P}^{422}$	^{410}PEHPAETE$\mathbf{Y_P}$DSL$\mathbf{Y_P}$PEDDL^{427}
$\mathbf{Y_P}^{418}Y^{422}$	^{410}PEHPAETE$\mathbf{Y_P}$DSLYPEDDL^{427}
$Y^{418}\mathbf{Y_P}^{422}$	^{410}PEHPAETEYDSL$\mathbf{Y_P}$PEDDL^{427}
$Y^{418}Y^{422}$	^{410}PEHPAETEYDSLYPEDDL^{427}

^{1}H and ^{31}P NMR Sample Preparation and Analysis. Approximately a 1:10 ratio of bovine thrombin to peptide was maintained for each complex studied. Sample preparation and analysis procedures similar to those of Trumbo and Maurer were employed (*36*). Selective features are summarized here. Each 400 μL NMR sample contained 1.5 mM peptide and either 0 or 151−162 μM bovine thrombin. The samples were buffered in 25 mM H_3PO_4, 150 mM NaCl, 0.2 mM EDTA, pH 5.6, and 10% D_2O (NMR buffer). Human γ-thrombin (Haematologic Technologies, Inc.) at 56 μM was buffer exchanged into the NMR buffer and concentrated to 153 μM via ultracentrifugation. With addition of the $Y_P^{418}Y_P^{422}$ peptide, the final ratio of γ-thrombin to peptide was 1:11 in 10% D_2O.

All ^{1}H NMR experiments were performed on either a Varian Inova 800 MHz spectrometer equipped with a triple resonance probe and pulsed-field triple axis gradients or a Varian Inova 500 MHz spectrometer equipped with a triple resonance probe and pulsed-field *z*-axis gradients. Two-dimensional transferred NOESY experiments of the enzyme−peptide complexes were run at 15 or 17 °C with 32 transients, 512 t_1 increments, a mixing time of 400 ms, and a spectral width of 8006 or 5006 Hz. Spectra were processed using FELIX2000 software (Accelerys, San Diego, CA) on a Silicon Graphics Octane workstation. For ^{31}P NMR, spectra were recorded on a Varian Inova 500 MHz spectrometer equipped with a 5 mm broad-band probe tuned to 202.4 MHz. The spectra were referenced to the peak corresponding to H_3PO_4 (0.00 ppm).

HDX Sample Preparation. Aliquots of 100 μL of 142−150 μM thrombin were buffer exchanged and diluted into 75 mM NaCl and 12.5 mM NaH_2PO_4, pH 6.5 (HDX Buffer), with Amicon-Ultra 4 units (10000 MWCO). The final target concentration of thrombin for all HDX preparations was from 20 to 25 μM. PPACK-inhibited thrombin was prepared by adding 5 μL of 11 mM PPACK to a thawed thrombin sample diluted to 545 μL with the HDX buffer (resulting in a 4:1 ratio of PPACK to thrombin). The PPACK-inhibited thrombin solution was incubated at 37 °C for at least 30 min. An assay involving the chromogenic substrate S2238 was employed to establish that thrombin was inactivated by PPACK. Following inactivation, PPACK-inhibited thrombin was buffer exchanged in the same manner as active thrombin. For samples containing the γ' peptide, 25 μL of 480 μM γ' peptide in deionized water was added to 24 μL of the buffer-exchanged thrombin (20−25 μM). The aliquots of the buffer-exchanged thrombin, with and without the peptide, were evaporated to dryness using a SpeedVac unit (Savant). The dry aliquots were stored at −70 °C.

HDX Experiments. Dry aliquots of thrombin or $Y_P^{418}Y_P^{422}$ peptide−thrombin were allowed to come to room temperature before the experiment was begun. Twelve microliters of 99.996% D_2O (Cambridge Isotope Laboratories) was added to the aliquot, yielding the final concentrations: 40−

50 μM thrombin/PPACK-inhibited thrombin, with or without 1000 μM γ′ peptide, in 150 mM NaCl and 25 mM NaH_2PO_4, pH 6.5. The samples were incubated in a desiccator at room temperature for 1 or 10 min. An initial set of HDX experiments were performed for 1 min with varying concentrations of the γ′ peptide (150−1500 μM) to determine the target peptide concentration and to address the possibility of nonspecific binding interactions.

Since thrombin possesses four disulfide bonds, both a reducing and nonreducing digest was necessary to produce maximal sequence coverage. First, deuterium exchange was quenched by adding 114 μL of 0.1% trifluoroacetic acid (TFA) (on ice) to acidify (pH 2.5) the solution. Immediately, 66 μL was transferred to a tube of activated pepsin bound to 6% agarose (Pierce Chemical Co.). To the remaining quenched thrombin was introduced 6 μL of 1 M TCEP [tris-(2-carboxyethyl)phosphine hydrochloride; Pierce Chemical Co.], the resultant solution was quickly vortexed, and the entire solution was added to another tube of activated pepsin. After deuteration, the entire process of splitting thrombin into a nonreducing and reducing pepsin digest took 30−40 s. Digestion occurred on ice for 10 min. Centrifugation at 4 °C separated the digest from the pepsin, and 10 μL aliquots were immediately frozen in liquid nitrogen and stored at −70 °C.

HDX Analysis. A frozen HDX aliquot of thrombin, with or without peptide, was thawed and immediately mixed with an equal volume of 10 mg/mL α-cyanohydroxycinnamic acid matrix (Aldrich) in 1:1:1 ethanol/acetonitrile/0.1% TFA, pH 2.2, and then 0.5 μL was spotted onto a chilled stainless steel MALDI plate. The spotted MALDI plate was dried within a SpeedVac unit (Savant) and inserted into the MALDI-TOF MS. The amount of time required for the plate to dry was roughly equivalent to the time needed for the MALDI-TOF MS to cycle through the eject protocol and accept the plate for analysis. The entire procedure took about 5 min of time, limiting the amount of hydrogen back-exchange. The spectra were collected in the reflector mode over a mass range of *m*/*z* 800−3500 with 256 laser shots per spectrum. All peptides in the peptic digest were previously identified by Croy and co-workers and verified in the current studies by in-house post source decay sequencing (*37*). Additional peptides obtained from the reduction of thrombin by TCEP were identified in-house with additional assistance from Julia Koeppe employing a MALDI TOF/TOF MS (University of California at San Diego). The program Data Explorer (Applied Biosystems) was used to analyze the spectra. Calibration of the spectra involved two reference peptides, one with the singly protonated monoisotopic mass of 888.4943 Da (residues 46−52) and the other with the singly protonated pentaisotopic mass of 2106.1505 Da (residues 85−99).

The amount of deuterium uptake by each peptide was quantified using the equation:

$$I_m = \sum_{i=1}^{n}[(x_i/\sum_{i=1}^{n}x_i)m_i]$$

where I_m represents the average mass of the isotopic cluster (also termed centroid), x_i is the intensity of peak *i* within the isotopic cluster, and m_i is the mass of peak *i*. The summation encompasses all peaks in a cluster that have signal to noise ratios of at least 2. By subtracting the undeuterated centroid from each deuterated centroid, the amount of deuterium incorporated into the specified peptide is quantified. At least three spectra were collected during each trial, and three trials were run for each time point under each condition. Results obtained were comparable to previously used methods employing the CAPP (Centroid APPlication Program) (*37*−*40*).

Quantification of differences in deuteration between thrombin in the absence and presence of ligands was calculated using the equation:

$$\%\ \text{difference} = [(D - D_{IIa})/D_{max}] \times 100$$

where *D* is the amount of deuterium incorporated in the presence of ligand (γ′ peptide, PPACK, or γ′ peptide/PPACK), D_{IIa} is the amount of deuterium incorporated for free thrombin (IIa), and D_{max} is the theoretical maximum amount of deuterium incorporation within the indicated peptide. Based on previous HDX data analysis, only percent differences greater than 4.5% are considered to be of great significance (*41*−*43*). The theoretical maximum number of exchangeable protons accounts for all exchangeable backbone amide protons and a slight fraction of N-terminal, C-terminal, and side chain exchangeable protons which are dependent on the final percentage of D_2O in solution under quench conditions (approximately 4.5%).

RESULTS

One-Dimensional Line Broadening NMR. One-dimensional proton NMR spectra of the different fibrinogen γ′ peptides were obtained in the absence and presence of thrombin. The appearance of resonance broadening in the spectra is indicative of peptide protons coming in direct contact with the thrombin surface. Figure 2 illustrates the extensive binding interactions observed for the $Y_P^{418}Y_P^{422}$ peptide. Widespread line broadening is observed for the entire 1D spectrum, including the NHs spanning residues H^{412} to L^{427}, the β, δ, and ε protons of Y_P^{418} and Y_P^{422}, the β protons of D^{419}, D^{425}, and D^{426}, and the β, γ, and δ protons of residues L^{421} and L^{427}. Only three observable proton resonances in Figure 2 remain unchanged with the addition of the enzyme: P^{410} β, E^{411} NH, and H^{412} δ. One-dimensional NMR of the $Y_P^{418}Y_P^{422}$ peptide and γ-thrombin containing an impaired ABE-I site displayed similar widespread line broadening (data not shown).

To assess the contributions that each phosphotyrosine makes to the interaction with thrombin, singly phosphorylated peptides were also analyzed. The spectrum for the Y_P^{422} peptide indicates broadened peaks for several residues (Figure S1 in Supporting Information). These spectra provide evidence that phosphorylation at a single tyrosine is sufficient to promote binding of the γ′ peptide to ABE-II. The absence of the phosphate at Y^{418}, however, abrogates enzyme contact for, at the least, the protons H^{412} NH, A^{414} NH and β, T^{416} γ, Y^{418} ε, and L^{421} γ and δs.

With the Y_P^{418} peptide, the appearance of much weaker enzyme binding is evident when examining the spectra in Figure S2, suggesting that most protons are not contacting the surface of the enzyme. The only significant amount of line broadening that can unambiguously be assigned is

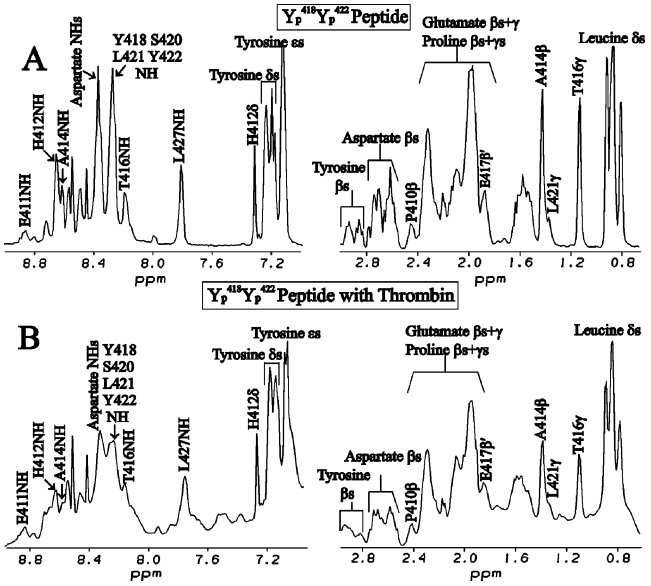

FIGURE 2: Line broadening in 1D proton NMR spectra for the $Y_P^{418}Y_P^{422}$ peptide in the presence of thrombin. (A) Spectrum for 1.5 mM peptide in solution. (B) Spectrum for 1.5 mM peptide in the presence of 0.162 mM thrombin. All NMR samples are in 25 mM H_3PO_4, 150 mM NaCl, 200 μM EDTA, and 10% D_2O, pH 5.6 (NMR buffer). All observable protons make extensive contact with the surface of thrombin except P^{410} β, E^{411} NH, and H^{412} δ.

observed for the following protons: A^{414} β, E^{417} NH and β', Y^{418} δ and ϵ, and D^{419}, D^{425}, and D^{426} βs. The amide region of the Y_P^{418} spectra also displays broadening for a peak that includes the NH of H^{412}, A^{414}, and E^{424}, indicating that all three of these amide protons are contacting the surface of thrombin. To complete the series, 1D spectra of the unphosphorylated peptide were obtained which lacked any line broadening in the presence of thrombin (data not shown).

Two-Dimensional Transferred Nuclear Overhauser Effect NMR. For the γ' peptides representing $Y_P^{418}Y_P^{422}$, Y_P^{418}, and Y_P^{422}, between 135 and 155 interresidue NOEs were observed in the presence of thrombin displaying similar structural features. By removing both phosphates from the peptide, 26 interresidue NOEs were identified. This significant decrease in NOEs suggests that phosphorylation of at least one tyrosine residue is required for interacting effectively with thrombin. Such an effect is in agreement with the 1D line broadening studies.

Important structural information related to the conformation of all three phosphorylated peptides bound to thrombin was obtained through analysis of the tr-NOESY spectra. Key through-space interactions were observed between H^{412} α and P^{413} δs, as well as Y^{422} β and P^{423} δs. These NOEs are indicative of an Xxx−Pro bond in the trans conformation (*44*). Figure 3 from a tr-NOESY spectrum of Y_P^{418} displays a β-turn between residues Y^{422} and D^{425}. The principal NOEs for this turn are between the P^{423} α and E^{424} NH, the P^{423} α and D^{425} NH, and the NHs of E^{424} and D^{425} (*44*). The NOEs for the β-turn and the proline trans bonds were also present in the 2D spectrum of γ-thrombin and the $Y_P^{418}Y_P^{422}$ peptide (data not shown). Examining the tr-NOESY spectrum for the unphosphorylated peptide with native thrombin reveals the existence of a H^{412}−P^{413} trans bond, but the required NOEs for the β-turn and the C-terminal proline trans bond are not present. A region

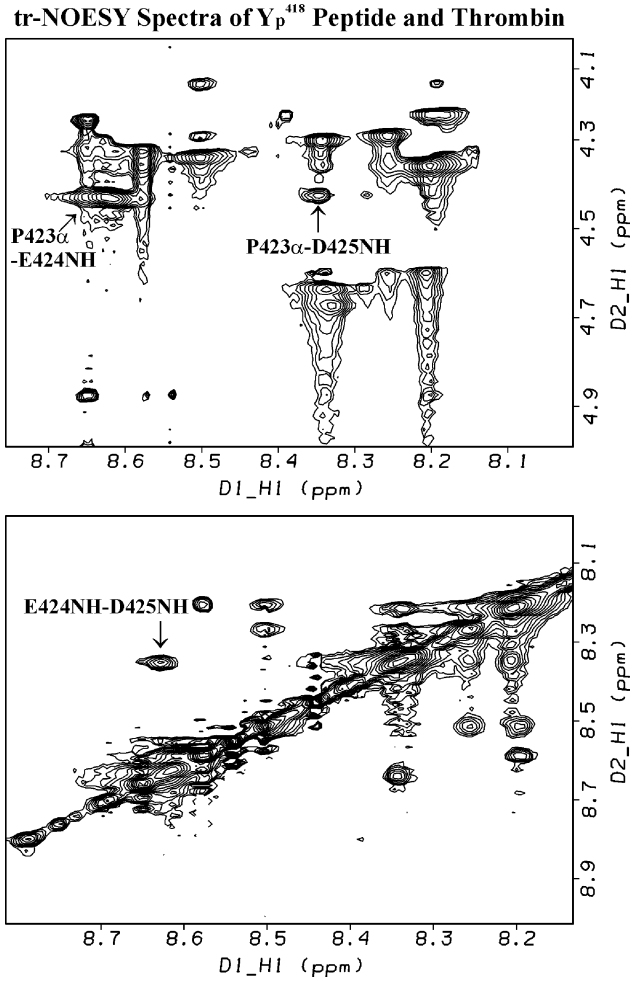

FIGURE 3: Representative 2D transferred NOESY spectrum of the β-turn between residues Y^{422}−D^{425} from the Y_P^{418} peptide (1.5 mM) in the presence of thrombin (0.151 mM). All three phosphorylated peptides exhibit this conformational feature, while the turn is absent when analyzing spectra involving the nonphosphorylated peptide.

displaying numerous proton interactions in the tr-NOESY spectra of the three phosphorylated peptides is centered around the two aromatic tyrosine residues (Figure 4). A hydrophobic cluster, or an intense grouping of aliphatic protons, is present encompassing residues T^{416} to D^{425}. By including through-space interactions between E^{424} α and the aliphatic chain of L^{427}, this cluster extends to the C-terminus of the peptide (data not shown).

^{31}P NMR Studies. Phosphorus NMR spectra were collected for the $Y_P^{418}Y_P^{422}$, Y_P^{418}, and Y_P^{422} peptides with and without thrombin in solution. These experiments were performed to monitor the effects of peptide−enzyme interaction on line broadening. The $Y_P^{418}Y_P^{422}$ peptide displayed two distinct resonances at −3.06 and −3.14 ppm (Figure 5). Addition of thrombin resulted in a merging of both phosphorus signals into one peak with a significant amount of line broadening. The singly phosphorylated peptides were also analyzed to assess the contribution each individual phosphotyrosine makes to the ^{31}P NMR spectrum. The Y_P^{418} and Y_P^{422} peptide signals shift upfield with introduction of the enzyme. In both cases, the peaks are slightly broader, indicating interactions at the enzyme surface (data not shown).

HDX Experiments: Examining the Influence of the $Y_P^{418}Y_P^{422}$ Peptide on the Solvent Accessibility of Thrombin.

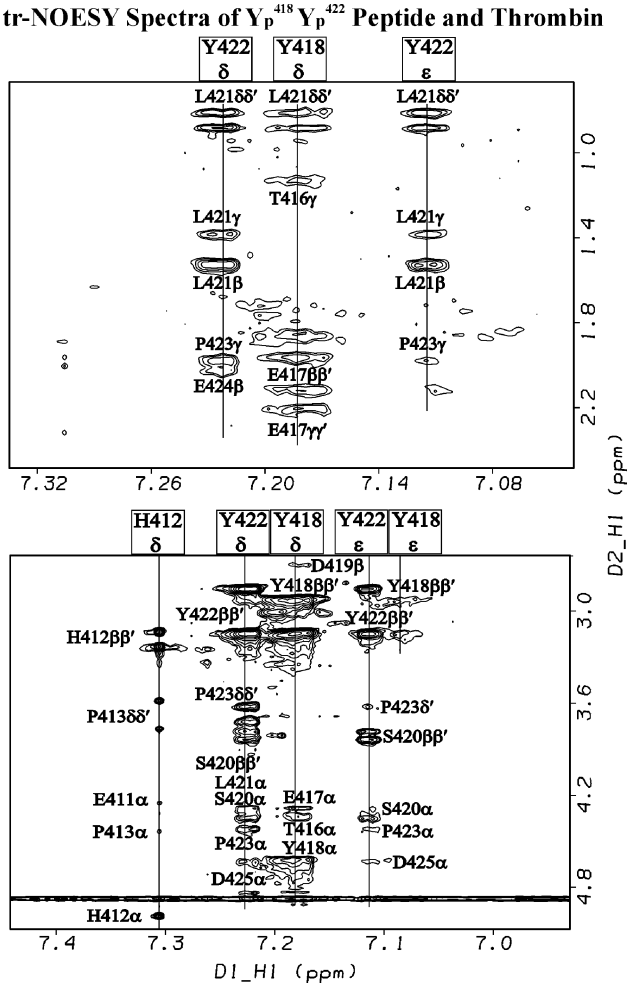

FIGURE 4: Representative 2D transferred NOESY spectrum of the intense clustering of NOEs centered around the aromatic protons of both tyrosine residues. The spectrum is from the tr-NOESY of the $Y_P^{418}Y_P^{422}$ peptide (1.5 mM) in the presence of thrombin (0.162 mM). The aromatic protons of Y^{418} are in close proximity to aliphatic protons from T^{416}, E^{417}, D^{419}, and L^{421}, while the Y^{422} ring protons display NOEs with residues S^{420}, L^{421}, P^{423}, E^{424}, and D^{425}. When the unphosphorylated peptide is observed, the NOEs are no longer present.

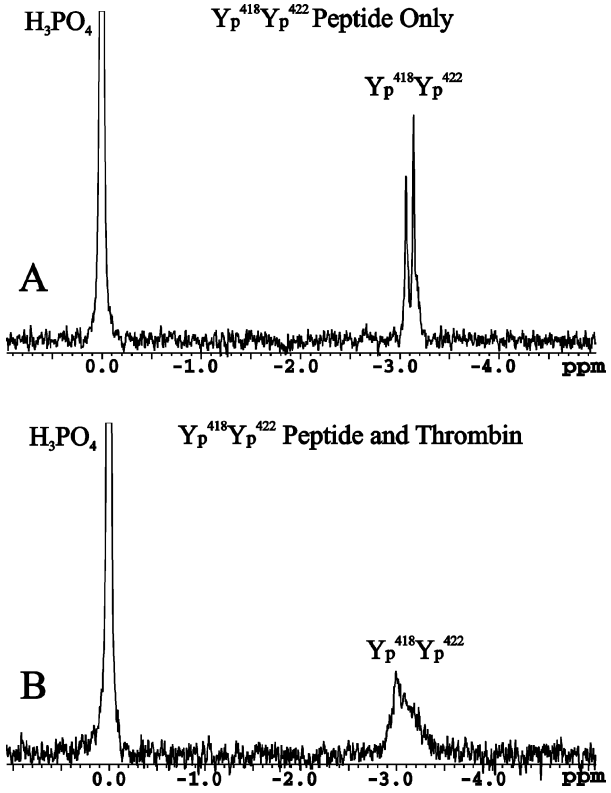

FIGURE 5: ^{31}P NMR spectra for the $Y_P^{418}Y_P^{422}$ peptide in the presence of thrombin. (A) Spectrum for 1.5 mM peptide in solution. (B) Spectrum for 1.5 mM peptide in the presence of 0.162 mM thrombin. Both phosphotyrosines are contacting the enzyme surface, resulting in a slight downfield shift of the broadened peak.

FIGURE 6: Sequence coverage from the peptic digest of bovine thrombin. Quantifiable peptide clusters obtained without a reducing agent are identified by solid black lines, while dashed lines refer to peptides acquired in the presence of TCEP. This coverage represents 44% of the total sequence and includes residues from both anion binding exosites, the W^{148} loop, the Na^+ binding site, and several residues involved in substrate specificity (L^{99}, I^{174}, and W^{215}). Residues in the catalytic triad are in green. ABE-I amino acids are in orange, and ABE-II residues are in red.

Peptic digests of thrombin, with and without the reducing agent TCEP, yielded 14 quantifiable isotopic clusters encompassing 44% of thrombin's sequence (Figure 6). The presence of four disulfide bonds (C^1−C^{122}, C^{42}−C^{58}, C^{168}−C^{182}, and C^{191}−C^{220}) limits the amount of sequence coverage attainable without introducing a reducing agent. Peptides spanning ABE-I (65−84), ABE-II (85−99), the autolysis loop (135−149D), and several residues involved in substrate specificity (L^{99} and I^{174}) are represented in the peptic digests. TCEP allowed for additional coverage to be obtained in the A-chain (−3 to 7), as well as a region encompassing W^{215} and the Na^+ binding site (212−227).

A series of 1 min HDX trials was performed to examine thrombin and PPACK-inhibited thrombin in complex with increasing concentrations of the γ′ peptide (150−1500 μM). These experiments were used to verify the target γ′ peptide concentration for this series of experiments. In addition, it would be possible to screen for secondary or nonspecific interactions to another thrombin region. In all cases, the protection from solvent for each thrombin and PPACK-inhibited thrombin derived peptide followed a similar transition across the 150−1500 μM γ′ peptide concentration range. Also, the results indicated that γ′ peptide concentrations of up to 1.5 mM are likely not high enough to promote secondary binding to ABE-I. For both thrombin and PPACK-inhibited thrombin, the γ′ peptide concentration was kept at 1 mM since higher concentrations did not result in any significant variance in the deuteration profiles of thrombin isotopic clusters. The resulting concentration of 1 mM γ′ peptide provided at least 99.93% occupancy of 40−50 μM thrombin (K_D = 0.68 μM) (*10*).

Thrombin with or without the addition of 1 mM γ′ peptide was exposed to 100% D_2O for either 1 or 10 min. The raw data representing total deuterium incorporation for thrombin

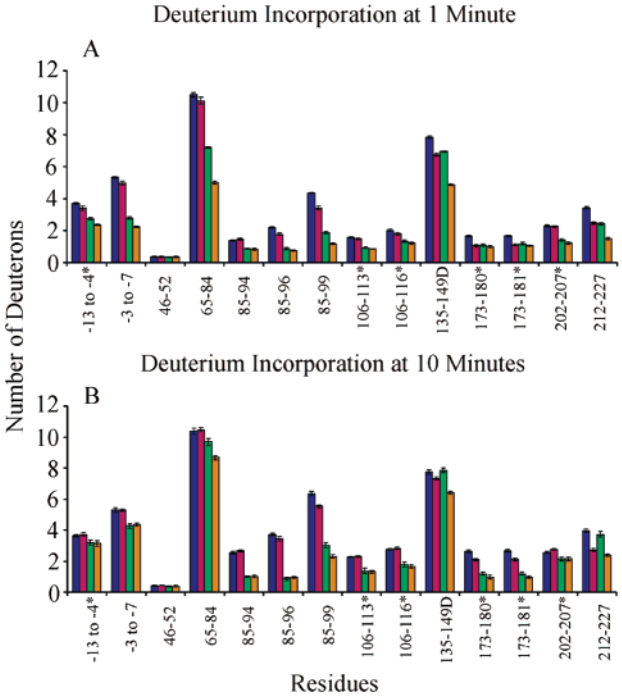

FIGURE 7: Graph of deuterium incorporation at 1 min (A) and 10 min (B) for thrombin in the absence or presence of ligands. The bars in the graph correspond to the following conditions: thrombin alone (purple), PPACK-inhibited thrombin (magenta), γ' peptide bound to thrombin (green), and γ' peptide bound to PPACK-inhibited thrombin (orange). The asterisk symbol (*) refers to data obtained in the absence of TCEP. Errors correspond to standard deviation of the mean for three independent experiments.

are available in Supporting Information (Table S1) and depicted graphically in Figure 7. On the basis of affinity for thrombin, only the $Y_P^{418}Y_P^{422}$ peptide was used in the HDX work. The 14 quantifiable peptides represent 10 distinct regions within thrombin. When analyzing thrombin without the presence of any ligands, five of these regions were continuing to exchange for deuterium after 10 min: 85−99, 106−116, 173−181, 202−207, and 212−227 (Figure 7, Table S1). These residues span ABE-II, the Na^+ binding site, and the substrate specificity residues L^{99}, I^{174}, and W^{215}. The other five segments, representing ABE-I, the A-chain, and the autolysis loop, became saturated with deuterium at 1 min: −13 to −4, −3 to 7, 46−52, 65−84, and 135−149D. The continued uptake of deuterium over the entire observed time range is specific to amide protons more protected from the solvent, or partially solvent exposed, such as residues involved in substrate recognition near the active site. Conversely, almost complete initial saturation of the peptide indicates a more solvent-exposed region, as observed for the A-chain and the autolysis loop (*45*).

Back-exchange from deuterium to hydrogen resulting from humidity, the addition of quench solutions, and matrix accounted for a 50% loss of deuterium during the allotted experimental time. This was determined by performing the HDX protocol on a small model peptide. The amount of back-exchange is essentially constant for each individual peptide, verified by the low standard deviation for three independent trials. Only differences in percent deuteration between two states of the protein are desired; therefore, a correction for deuterium loss was not necessary.

Differences in Deuteration between Thrombin and the $Y_P^{418}Y_P^{422}$ Peptide−Thrombin Complex. The γ' peptide imparts a significant amount of solvent protection from D_2O (Table 3, Figure 7) in five thrombin peptides representing two regions within ABE-II. Peptides 85−94 (*m*/*z* 1317.73), 85−96 (*m*/*z* 1617.86), and 85−99 (*m*/*z* 2102.12) are situated in the center of ABE-II. Peptides 173−180 (*m*/*z* 1018.56) and 173−181 (*m*/*z* 1165.63) involve peripheral ABE-II residues and the substrate specificity residue I^{174}. After 10 min of deuteration, the negative percent differences for these ABE-II regions significantly increased compared to 1 min (Table 3). For example, residues 85−94 are protected by 0.5 deuteron at 1 min (−5.6%) and then by 1.6 deuterons at 10 min (−17.7%) as the γ' peptide binds to ABE-II (Figure 8B,D versus Figure 8G,I).

In addition to the noted protection within the vicinity of ABE-II, the γ' peptide also shielded regions distant from ABE-II. Unlike the ABE-II fragments, these thrombin segments lost some of their degree of protection as the incubation with D_2O was increased from 1 to 10 min. Such thrombin segments are likely not becoming completely solvent excluded in the presence of the γ' peptide. The regions affected include ABE-I (65−84 and 106−116), the A-chain (−13 to −4 and −3 to 7) and a nearby B-chain loop (202−207), the W^{215} region (212−227), and the autolysis loop (135−149D). See Table 3 and also Figure 7. Panels B and D of Figure 9 illustrate that within 1 min the

Table 3: Changes in Percent Deuteration for Thrombin−Ligand Complexes at 1 and 10 min Relative to Free Thrombin[a]

		P-IIa[e]		γ'−IIa		γ' P−IIa	
residues	theo D_{max} [b]	1 min	10 min	1 min	10 min	1 min	10 min
−13 to −4[c]	8.5	−3.6	0.8	**−11.3**	**−5.1**	**−15.9**	**−5.8**
−3 to 7	16.9	−2.0	0.0	**−15.0**	**−6.1**	**−18.2**	**−5.6**
46−52	6.6	0.0	0.0	−0.2	−0.7	0.1	−0.6
65−84	21.8	−1.6	0.4	**−15.1**	−3.3	**−25.1**	**−7.9**
85−94	8.8	1.1	1.2	**−5.6**	**−17.7**	**−6.2**	**−17.6**
85−96	10.9	−3.9	−2.5	**−12.3**	**−25.9**	**−13.4**	**−25.2**
85−99	15.2	**−6.3**[d]	**−5.5**	**−16.4**	**−21.8**	**−20.9**	**−26.6**
106−113[c]	6.7	−1.6	−0.5	**−10.0**	**−13.1**	**−10.8**	**−13.9**
106−116[c]	9.8	−2.1	−0.6	**−6.9**	**−10.0**	**−8.3**	**−11.2**
135−149D	19.4	**−5.5**	−2.2	**−4.6**	−0.5	**−15.2**	**−6.9**
173−180[c]	7.8	**−7.7**	**−7.0**	**−7.3**	**−18.6**	**−8.7**	**−21.3**
173−181[c]	8.8	**−6.6**	**−6.6**	**−5.9**	**−16.9**	**−7.1**	**−19.3**
202−207[c]	6.8	0.5	2.9	**−13.2**	**−6.1**	**−15.8**	**−6.1**
212−227	15.9	**−6.0**	**−7.9**	**−6.3**	−1.5	**−12.1**	**−10.0**

[a] The % change for a particular peptide is calculated by the equation, % difference = $[(D - D_{IIa})/D_{max}] \times 100$, where D is the amount of deuterium incorporated in the presence of ligand (γ' peptide, PPACK, or γ' peptide/PPACK), D_{IIa} is the amount of deuterium incorporated in the absence of ligands, and D_{max} is the theoretical maximum number of exchangeable protons within the indicated peptide. [b] The maximum number of exchangeable protons within the indicated peptide, assuming 100% deuteration. This value accounts for all exchangeable backbone amide protons and a slight fraction of N-terminal, C-terminal, and side chain exchangeable protons which are dependent on the final percentage of D_2O in solution under quench conditions (approximately 4.5%). A fully deuterated peptide would theoretically have acquired this amount of deuterons. [c] The deuterium uptake for these peptides was quantified from the nonreducing digests. All other peptides are from the digests with TCEP. When isotopic clusters appear in both the TCEP and non-TCEP digests, the differences in deuteration are negligible when comparing similar peptides. Certain peptides appear exclusively under nonreducing or reducing conditions, hence the necessity of performing both types of peptic digests. [d] The values in bold represent significant changes in deuteration of greater than −4.5%. [e] Abbreviations: IIa, thrombin; P-IIa, PPACK-inhibited thrombin; γ'−IIa, γ' peptide bound to thrombin; γ' P−IIa, γ' peptide bound to PPACK-inhibited thrombin.

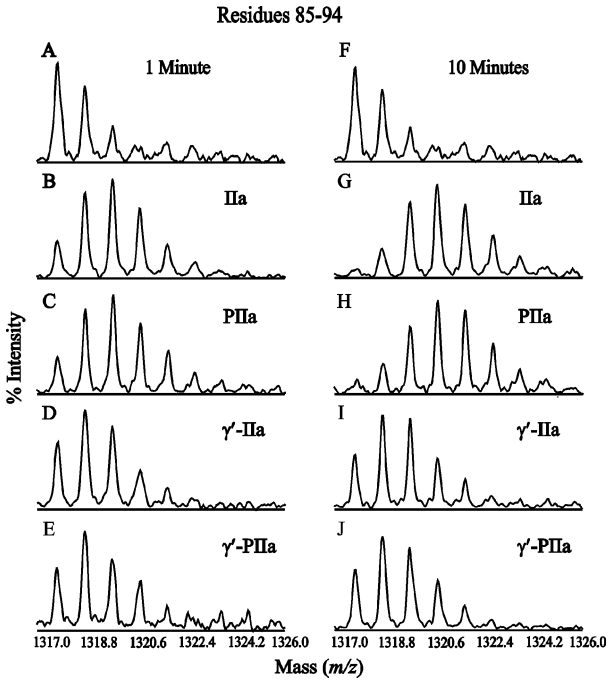

FIGURE 8: Mass spectra representing residues 85−94 (*m*/*z* 1317.73) after 1 and 10 minutes of deuteration. All D-on experiments are in 150 mM NaCl and 25 mM NaH_2PO_3, pH 6.5 (HDX buffer). Panels: (A and F) the undeuterated peak cluster, (B and G) thrombin spectrum in the absence of ligands, (C and H) PPACK-inhibited thrombin, (D and I) γ′ peptide bound to thrombin, and (E and J) γ′ peptide bound to PPACK-inhibited thrombin. This peak cluster contains the ABE-II residue R^{93} and experiences a significant degree of protection from deuterium in the presence of the γ′ peptide. This protection from solvent is maintained over the course of 10 min.

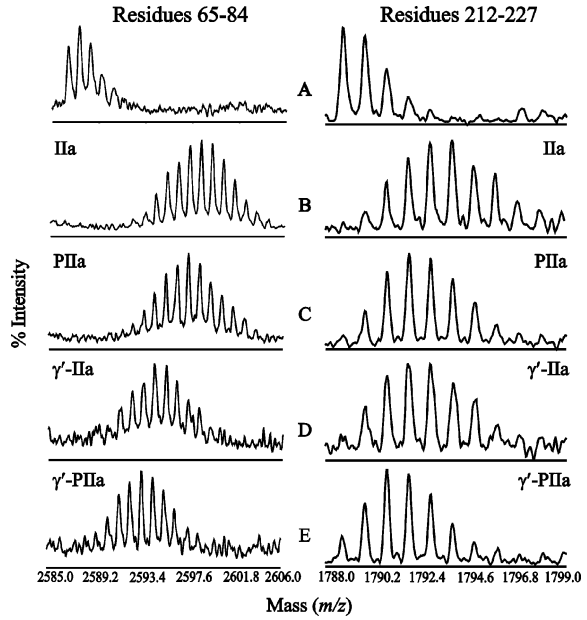

FIGURE 9: Mass spectra representing residues 65−84 (*m*/*z* 2586.48) and 212−227 (*m*/*z* 1718.80) after 1 min of deuteration. All D-on experiments are in 150 mM NaCl and 25 mM NaH_2PO_3, pH 6.5 (HDX buffer). Panels: (A) the undeuterated peak cluster, (B) thrombin spectrum in the absence of ligands, (C) PPACK-inhibited thrombin, (D) γ′ peptide bound to thrombin, and (E) γ′ peptide bound to PPACK-inhibited thrombin.

isotopic cluster representing residues within ABE-I (65−84) underwent a −15.1% difference in deuteration relative to free thrombin whereas the cluster for residues within the W^{215} region (212−227) underwent a −6.3% difference. The only fragment of thrombin which remained insensitive to the γ′ peptide binding to ABE-II was residues 46−52.

Differences in Deuteration between PPACK-Inhibited Thrombin and the $Y_P^{418}Y_P^{422}$ Peptide−PPACK-Inhibited Thrombin Complex. Introduction of the γ′ peptide to PPACK-inhibited thrombin resulted in at least −4.5% protection from deuteration for almost every affected region of thrombin (Tables 3 and S1, Figure 7). After 10 min of deuteration, the peptide 85−99 (*m*/*z* 2102.12) experiences a decrease in deuteration of −21.8% in the presence of the γ′ peptide and a decrease of −5.5% with PPACK bound to the active site, and both interacting together with thrombin result in a decrease of −26.6% (Table 3). These additive shifts lead to lower *m*/*z* values for the peptide as can be seen by comparing the isotopic clusters of PPACK-inhibited thrombin, γ′ peptide−thrombin, and γ′ peptide−PPACK-inhibited thrombin.

Located adjacent to this ABE-II region is the fragment 173−181. This segment encompasses several residues involved in substrate specificity (R^{173} and I^{174}) and some peripheral ABE-II residues (R^{173} and R^{175}). When examining the data for 1 min of deuteration, the binary and ternary complexes with thrombin offer similar degrees of protection (between −5.9% and −7.1%) (Table 3). After 10 min of deuteration, differences are observed across the series of complexes. γ′−thrombin exhibits a value of −16.9%, PPACK-inhibited thrombin a value of −6.6%, and γ′−PPACK-inhibited thrombin a value of −19.3% (Table 3). The γ′ peptide appears capable of imparting an increasing degree of protection over 10 min whereas PPACK's effect diminishes.

Another region of thrombin for which there are some time-dependent trends in deuteration involves residues 212−227. This peptide includes W^{215}, a critical residue involved in substrate specificity that previously could not be monitored. Shifts to this peptide's isotopic cluster can be followed in Figure 9B−E, Tables 3 and S1, and Figure 7. After 1 min of deuteration, both PPACK-inhibited thrombin and γ′ peptide−thrombin impart a similar degree of protection from solvent (−6.0% and −6.3%). Protection of the ternary γ′ peptide−PPACK-inhibited thrombin complex appears additive at −12.1%. Similarities in protection for the binary complexes, however, are lost for the 10 min deuteration point. PPACK-inhibited thrombin now exhibits protection of −7.9%, whereas γ′ peptide no longer significantly affects this region (−1.5%). Interestingly, the degree of protection of the ternary complex is still roughly additive at −10.0%. Contrary to results for segment 173−181, it is the PPACK, not the γ′ peptide, which dominates in hindering exchange for segment 212−227.

Two solvent-exposed regions encompassing ABE-I and the autolysis loop present evidence of a synergistic effect involving the interactions of both ligands. For example, after 1 min of deuteration for residues 65−84, the presence of PPACK affords very little protection from solvent (−1.6%) (Figure 9C), the γ′ peptide provides significant protection (−15.1%) (Figure 9B), and both together offer even more protection from solvent than an additive effect would suggest (−25.1%) (Figure 9D). The same is true for the segment spanning 135−149D (Table 3). The presence of both of these ligands appears to stabilize these surface regions of thrombin,

protecting the backbone amides from exchange more effectively than either ligand acting alone.

The peptides spanning residues −13 to 7, 106−116, and 202−207 experienced roughly similar protection when the γ′ peptide bound to ABE-II in the presence or absence of PPACK. PPACK's sphere of influences must not extend to these fragments. The A-chain peptides −13 to −4 (*m*/*z* 1254.54) and −3 to 7 (*m*/*z* 1924.92) incorporate an almost identical amount of deuterium at 1 min and after 10 min display similar percent differences (ranging from −5.1% to −6.1%) (Table 3). Located in close proximity to the A-chain, the fragment 202−207 (*m*/*z* 1064.53) was also protected from solvent within 10 min of deuteration by a comparable amount to the A-chain (−6.1%) (Table 3). Finally, peptides 106−113 (*m*/*z* 996.66) and 106−116 (*m*/*z* 1311.80), containing several peripheral ABE-I residues, incorporated virtually identical amounts of deuterium regardless of the presence of PPACK (Tables 3 and S1).

DISCUSSION

The binding interface for the γ′ peptide has been localized to thrombin anion binding exosite II (*10*, *11*). Additional information is needed on the conformational features the peptide adopts upon binding and the contribution each sulfotyrosine makes toward the thrombin interaction. There is also interest in determining the residues within thrombin ABE-II that make contact with the peptide and the possible long-range effects associated with a binding event at this exosite. The current work employs solution NMR methods and HDX coupled with MALDI-TOF mass spectrometry to further describe the γ′ peptide−thrombin relationship.

Analysis of NMR Data: Insight into the Structural Requirements for the γ′ Peptide Interaction with Thrombin's Anion Binding Exosite II. One-dimensional ^{1}H and ^{31}P NMR demonstrate that the $Y_P^{418}Y_P^{422}$ peptide makes significant contact with the thrombin surface (Figures 2 and 5). The NMR broadening effects are in agreement with observations that truncation of the γ′ peptide from E^{411}−L^{427} to A^{414}−L^{427} decreases binding affinity almost 4-fold whereas peptides lacking the N-terminal residues P^{410}−T^{416} demonstrate no observable binding to ABE-II (*10*, *25*). The current work makes it possible to identify individual protons on amino acids that participate in this binding. The consequences of removing the phosphates were also screened using 1D ^{1}H and ^{31}P NMR line broadening. Figures S1 and S2 in Supporting Information demonstrate that both the Y_P^{418} and Y_P^{422} peptides are interacting with thrombin. The binding segment of the Y_P^{422} peptide exhibits more extensive contact with thrombin than the Y_P^{418} peptide, suggesting a more instrumental role for Y_P^{422} in anchoring the γ′ peptide segment to thrombin. Although phosphorylation at either position is enough to support the ABE-II interaction, the presence of both phosphates in the γ′ peptide promotes more effective binding to thrombin as evidenced by the increased line broadening.

Two-dimensional tr-NOESY spectra supply critical information regarding the conformational features the peptides adopt when interacting with thrombin. All three phosphorylated peptides generate similar spectra, illustrating that thrombin-bound structural characteristics are preserved as long as one phosphotyrosine is present. Key conformational features for the bound γ′ peptides include a β-turn between residues Y^{422} and D^{425}, a trans conformation adopted by both Xxx−Pro bonds, and a cluster of NOEs centered around the aromatic rings of both tyrosine residues. The Tyr groups and their neighbors are major contributors to establishing the bound structure. Our results demonstrate the requirement of at least one modified Tyr residue in the specific interaction of the γ′ chain and ABE-II.

One-Dimensional and Two-Dimensional NMR with γ-Thrombin: The γ′ Peptide Targets ABE-II. Previous solution studies have demonstrated that the primary binding site for the γ′ peptide is ABE-II (*10*, *11*). Recent crystal structures of GpIbα and thrombin display interactions occurring with both ABE-II and ABE-I (*46*, *47*). GpIbα and the γ′ peptide have quite a comparable clustering of Y_S, E, and D residues (Table 1). Therefore, 1D proton NMR and 2D tr-NOESY NMR spectra were obtained for the γ′ peptide in the presence of γ-thrombin to address if the peptide is interacting with ABE-I or influenced by this exosite. The γ variant of thrombin retains catalytic activity while possessing an impaired ABE-I due to cleavages after residues R^{75}/R^{77A} and K^{149E} (*48*). The spectra obtained were remarkably similar to the spectra obtained for wild-type thrombin, suggesting that the structural information results from interactions at ABE-II (data not shown).

Analysis of HDX Results. (I) Establishing the γ′ Peptide−Thrombin Binding Interface. HDX coupled with the MALDI-TOF MS was performed to gain further insight on the location of the γ′ peptide interface with thrombin. Observed decreases in deuteration could be the product of a restricted ensemble of conformations (protein stabilization), a conformational change, or a ligand−protein interface. When examining the HDX results, differences in deuteration at sites located within ABE-II are due primarily to the shielding of backbone amides from solvent by the γ′ peptide. Regions distant from the γ′ peptide−thrombin interface that display protection from the solvent are probably experiencing a change in dynamics due to binding at ABE-II.

As of yet, there are no reported X-ray crystal structures of the γ′ peptide−thrombin complex. A number of mutagenesis studies and crystallographic structures have demonstrated the importance of thrombin R^{93} and, to a lesser extent, R^{97} in ligand binding to thrombin ABE-II (*9*, *24*, *46*, *47*, *49*−*51*). The HDX data present evidence that the γ′ peptide is interacting with residues R^{93} and R^{97} (see Figures 1B and 10A), supporting previous work with thrombin mutants and the γ′ peptide (*10*). The γ′ peptide−thrombin NMR spectra demonstrate significant secondary structural features for residues Y_S^{418}−D^{425}, which may be centered at the heart of ABE-II (R^{93} and R^{101}). The role of R^{101}, however, could not be verified since the peptic digests of thrombin did not cover this residue. Furthermore, the HDX studies revealed that a portion of γ′ peptide located N-terminally to the β-turn could be positioned to interact near R^{97}, R^{173}, and R^{175}. Without complete coverage of ABE-II (namely, the C-terminal helix of thrombin), the possibility of interactions within residues R^{233}−K^{240} cannot be discounted. It is interesting to note that haemadin and prothrombin fragment 2 display turn structures that interact with R^{93}, R^{97}, R^{101}, R^{173}, and R^{175} (*9*, *49*).

There is evidence that binding of the γ′ peptide to thrombin ABE-II reduces the rate at which fibrinopeptide A (FpA) is released from fibrinogen and the chromogenic substrate

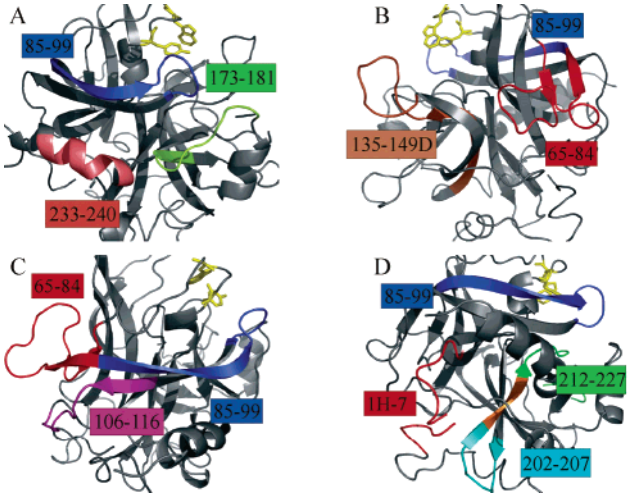

FIGURE 10: Four crystallographic views of PPACK-inhibited thrombin (1PPB). W^{60D} is in yellow. (A) ABE-II region 85−99 is in blue and 173−181 is in green. The additional ABE-II region not observed in the present HDX study, 233−240, is in pink. (B) The flexible solvent-exposed regions 65−84 (in red) and 135−149D (in brown). Both PPACK and the γ′ peptide significantly stabilize the segments upon ternary complex formation with thrombin. (C) Line of communication from ABE-II, 85−99 (in blue), to ABE-I, 65−84 (in red) and 106−116 (in purple). (D) The A-chain. There are several electrostatic contacts between the A-chain residues 1H−7 (in red) and the B-chain residues 202−207 (in teal). Also represented are 85−99 (in blue) and 212−227 (in green). The β-strand connecting 202−207 to 212−227 is in orange. These figures were created using PyMol (*4*).

S2238 is hydrolyzed (*52*). Contact of the γ′ peptide with the thrombin regions 85−99 and 173−181 could explain the hindered release of fibrinopeptide A. Crystal structures of FpA (7−16) and thrombin demonstrate the importance of R^{97}, E^{97A}, and I^{174} in orienting the peptide in the active site (*53*). HDX results indicate that peptide segments containing these residues are protected from deuteration in the presence of γ′ peptide. The γ′ chain could thus be hindering the helical turn of FpA from optimally accessing the active site region reducing the rate of catalysis (*11*, *54*). A similar suggestion has been offered for the inhibition of fibrinogen clotting activity by the chondrotin sulfate moiety of thrombomodulin (*51*).

Analysis of HDX Results. (II) Determining the Consequences of Ligand Binding to ABE-II on Several Key Regions of Thrombin. Binding of ligands (fibrinogen Aα, PAR1, thrombomodulin, and hirudin) to ABE-I has clearly been shown to affect reactivity within the thrombin active site region (reviewed in ref *55*). The reduced release of FpA from fibrinogen in the presence of γ′ peptide−thrombin (*52*) supports a linkage from ABE-II to the active site. Conflicting reports address the existence of an allosteric linkage between ABE-I and ABE-II (*54*, *56*). The current HDX studies provide evidence that ligand binding to ABE-II is perturbing the rate of deuterium exchange at other distant sites. The HDX results suggest lines of communication from ABE-II to a portion of ABE-I (Figure 10C), from ABE-II to a segment containing W^{215} (Figure 10D), and from ABE-II to a region of the A-chain (Figure 10D).

Interaction of the γ′ peptide with ABE-II resulted in a segment of ABE-I representing residues 65−84 to become more protected from solvent. A pathway from ABE-II to ABE-I can be traced from L^{99} back toward residue L^{65} as seen in Figure 10B. Electrostatic interactions between two antiparallel β-strands, including contacts between the residues E^{86}−K^{107}, K^{87}−K^{107}, and M^{84}−K^{109}, explain how an ABE-II binding event could be relayed to the peripheral ABE-I region involving residues 106−113 (*3*) (Figure 10C). A similar line of communication has been reported in a prior (*37*) and in our own HDX study of PPACK-inhibited thrombin. PPACK alone offers little protection for residues 85−96 (Table 3), while the observed protection within residues 97−99 is in part attributable to contacts with L^{99}. These PPACK interactions are proposed to be transmitted to ABE-I via the β-strand formed by residues 85−96 (*37*).

More information about sites of distant influence is revealed by examining the γ′ peptide−PPACK-inhibited thrombin complex. The ternary interactions resulted in a synergistic effect on the rate of deuterium exchange for the solvent-exposed regions 65−84 (ABE-I) and 135−149D (autolysis loop) (Figure 10B). This suggests that simultaneous binding of γ′ peptide and PPACK to thrombin significantly stabilizes these portions of the protease. Effects on the environment of region 212−227 are also important to consider. The additive effect observed for the ternary complex suggests that the two ligands may be independently influencing the solvent accessibility of region 212−227. The γ′ peptide could be affecting residues near W^{215} and/or other regions within the residues 212−227, while the D-Phe of PPACK is known to exhibit beneficial interactions with W^{215} via a perpendicular aryl−aryl arrangement (*3*).

In addition to altering the deuterium exchange dynamics for regions involving ABE-II, ABE-I, and the active site region, the γ′ peptide also exhibits effects on a portion of the thrombin A chain and a nearby B-chain fragment (202−207) (Figure 10D). As can be seen in Figure 10D, a simple direct connection cannot be made from ABE-II residues to the A-chain. Deletion of K^9 from the A-chain has recently been shown to perturb the pK_a of the catalytic residue H^{57}, slowing the catalytic activity of thrombin (*57*). This lysine residue contacts D^{1A} which is part of a segment that undergoes protection from solvent in the presence of the γ′ peptide. Since the γ′ peptide appears to only decrease k_{cat} values for the hydrolysis of the small chromogenic substrate S2238 (*52*), a direct consequence of the γ′ peptide binding to ABE-II may be to perturb the geometry of the catalytic triad affecting catalysis. Such perturbations to the active site might lead to a reverse line of communication back to the A-chain and the nearby B-chain segment (202−207).

Hydrogen−deuterium exchange studies on the binding of ligands to thrombin have revealed both local and long-range effects (*37*−*40*). The current work with the γ′ peptide illustrates lines of communication from ABE-II to ABE-I and from ABE-II to regions of the extended active site. Studies with PPACK-IIa display connections from the active site to similar regions of ABE-I and the edge of ABE-II (*37*). Binding of the thrombomodulin fragment TMEGF45 to thrombin ABE-I has led to perturbations in deuterium exchange within the 90s loop of ABE II (*39*, *40*). A distinct linkage between ABE-I and ABE-II may also have been demonstrated in earlier work involving a mixture of γ′ peptide, thrombin, and fibrin 1 (fibrinogen lacking the γ′ extension) (*25*). These different observations support the concept of an inter-exosite linkage reported between the two ABE-II binding ligands prothrombin fragment 2 and γ′

peptide and the ABE-I (*11*, *54*). On the contrary, another study with hirudin and heparin ligands did not observe as significant a negative allostery for the ABE-I/ABE-II connections (*56*). The HDX studies presented here cannot evaluate the extent to which inter-exosite linkages affect enzyme function, but they can establish potential lines of communication between the sites.

CONCLUSIONS

In this investigation, interactions between a series of γ' peptides and thrombin were characterized using solution NMR and HDX coupled with MALDI-TOF MS. One-dimensional NMR results indicate that residues H^{412}−L^{427} of the $Y_P{}^{418}Y_P{}^{422}$ peptide are responsible for the primary sites of contact with the thrombin surface and illustrate the importance of sulfonation at the Y^{422} position. Data from the 2D tr-NOESY spectra demonstrate that the ABE-II-bound γ' peptide adopts significant secondary structure in the presence of at least one phosphotyrosine. HDX results suggest that the γ' peptide interacts with thrombin ABE-II. In response to this binding, other regions of thrombin also experience protection from deuteration including ABE-I, regions near the active site, and a portion of the A-chain. Finally, thrombin can form a ternary complex with the γ' peptide and PPACK, generating an enzyme that is further stabilized from hydrogen−deuterium exchange.

ACKNOWLEDGMENT

We are grateful for the guidance and assistance of N. J. Stolowich, A. N. Lane, and S. Arumugam in carrying out the NMR experiments. We acknowledge the valuable contributions of B. T. Turner, Jr., in implementing the HDX protocol. Furthermore, we greatly appreciate the efforts of J. R. Koeppe (University of California at San Diego) in helping to identify the TCEP-derived peptides from thrombin. Finally, we extend much thanks to G. Isetti and D. B. Cleary for helpful discussions and critical evaluation of the present work.

SUPPORTING INFORMATION AVAILABLE

Table S1 displays the amount of total deuterium incorporation for thrombin at 1 and 10 min and Figures S1 and S2 illustrate line broadening for the $Y_P{}^{422}$ and $Y_P{}^{418}$ peptides in the presence of thrombin, respectively. This material is available free of charge via the Internet at http://pubs.acs.org.

REFERENCES

1. Di Cera, E. (2003) Thrombin interactions, *Chest 124*, 11S−17S.
2. Bode, W. (2005) The structure of thrombin, a chameleon-like proteinase, *J. Thromb. Haemostasis 3*, 2379−2388.
3. Bode, W., Turk, D., and Karshikov, A. (1992) The refined 1.9-Å X-ray crystal structure of D-Phe-Pro-Arg chloromethyl ketone-inhibited human alpha-thrombin: structure analysis, overall structure, electrostatic properties, detailed active-site geometry, and structure−function relationships, *Protein Sci. 1*, 426−471.
4. DeLano, W. L. (2002) *The PyMOL Molecular Graphics System*, DeLano Scientific, San Carlos, CA.
5. Olson, S. T., and Bjork, I. (1991) Predominant contribution of surface approximation to the mechanism of heparin acceleration of the antithrombin-thrombin reaction. Elucidation from salt concentration effects, *J. Biol. Chem. 266*, 6353−6364.
6. De Cristofaro, R., and De Filippis, V. (2003) Interaction of the 268−282 region of glycoprotein Ibalpha with the heparin-binding site of thrombin inhibits the enzyme activation of factor VIII, *Biochem. J. 373*, 593−601.
7. De Candia, E., Hall, S. W., Rutella, S., Landolfi, R., Andrews, R. K., and De Cristofaro, R. (2001) Binding of thrombin to glycoprotein Ib accelerates the hydrolysis of Par-1 on intact platelets, *J. Biol. Chem. 276*, 4692−4698.
8. Li, C. Q., Vindigni, A., Sadler, J. E., and Wardell, M. R. (2001) Platelet glycoprotein Ib alpha binds to thrombin anion-binding exosite II inducing allosteric changes in the activity of thrombin, *J. Biol. Chem. 276*, 6161−6168.
9. Richardson, J. L., Kroger, B., Hoeffken, W., Sadler, J. E., Pereira, P., Huber, R., Bode, W., and Fuentes-Prior, P. (2000) Crystal structure of the human alpha-thrombin-haemadin complex: an exosite II-binding inhibitor, *EMBO J. 19*, 5650−5660.
10. Lovely, R. S., Moaddel, M., and Farrell, D. H. (2003) Fibrinogen gamma′ chain binds thrombin exosite II, *J. Thromb. Haemostasis 1*, 124−131.
11. Pospisil, C. H., Stafford, A. R., Fredenburgh, J. C., and Weitz, J. I. (2003) Evidence that both exosites on thrombin participate in its high affinity interaction with fibrin, *J. Biol. Chem. 278*, 21584−21591.
12. Weisel, J. W. (2005) Fibrinogen and fibrin, *Adv. Protein Chem. 70*, 247−299.
13. Mosesson, M. W., Siebenlist, K. R., and Meh, D. A. (2001) The structure and biological features of fibrinogen and fibrin, *Ann. N.Y. Acad. Sci. 936*, 11−30.
14. Vali, Z., and Scheraga, H. A. (1988) Localization of the binding site on fibrin for the secondary binding site of thrombin, *Biochemistry 27*, 1956−1963.
15. Mosesson, M. W., Finlayson, J. S., and Umfleet, R. A. (1972) Human fibrinogen heterogeneities. 3. Identification of chain variants, *J. Biol. Chem. 247*, 5223−5227.
16. Wolfenstein-Todel, C., and Mosesson, M. W. (1980) Human plasma fibrinogen heterogeneity: evidence for an extended carboxyl-terminal sequence in a normal gamma chain variant (gamma′), *Proc. Natl. Acad. Sci. U.S.A. 77*, 5069−5073.
17. Kloczewiak, M., Timmons, S., Lukas, T. J., and Hawiger, J. (1984) Platelet receptor recognition site on human fibrinogen. Synthesis and structure−function relationship of peptides corresponding to the carboxy-terminal segment of the gamma chain, *Biochemistry 23*, 1767−1774.
18. Chung, D. W., and Davie, E. W. (1984) gamma and gamma′ chains of human fibrinogen are produced by alternative mRNA processing, *Biochemistry 23*, 4232−4236.
19. Fornace, A. J., Jr., Cummings, D. E., Comeau, C. M., Kant, J. A., and Crabtree, G. R. (1984) Structure of the human gamma-fibrinogen gene. Alternate mRNA splicing near the 3′ end of the gene produces gamma A and gamma B forms of gamma-fibrinogen, *J. Biol. Chem. 259*, 12826−12830.
20. Mosesson, M. W., and Finlayson, J. S. (1963) Biochemical and chromatographic studies of certain activities associated with human fibrinogen preparations, *J. Clin. Invest. 42*, 747−755.
21. Lovely, R. S., Falls, L. A., Al-Mondhiry, H. A., Chambers, C. E., Sexton, G. J., Ni, H., and Farrell, D. H. (2002) Association of gammaA/gamma′ fibrinogen levels and coronary artery disease, *Thromb. Haemostasis 88*, 26−31.
22. Bettelheim, F. R. (1954) Tyrosine-O-sulfate in a peptide from fibrinogen, *J. Am. Chem. Soc. 76*, 2838−2839.
23. Rydel, T. J., Tulinsky, A., Bode, W., and Huber, R. (1991) Refined structure of the hirudin-thrombin complex, *J. Mol. Biol. 221*, 583−601.
24. Sheehan, J. P., and Sadler, J. E. (1994) Molecular mapping of the heparin-binding exosite of thrombin, *Proc. Natl. Acad. Sci. U.S.A. 91*, 5518−5522.
25. Meh, D. A., Siebenlist, K. R., Brennan, S. O., Holyst, T., and Mosesson, M. W. (2001) The amino acid sequence in fibrin responsible for high affinity thrombin binding, *Thromb. Haemostasis 85*, 470−474.
26. Wolfenstein-Todel, C., and Mosesson, M. W. (1981) Carboxy-terminal amino acid sequence of a human fibrinogen gamma-chain variant (gamma′), *Biochemistry 20*, 6146−6149.
27. Dong, J. F., Li, C. Q., and Lopez, J. A. (1994) Tyrosine sulfation of the glycoprotein Ib-IX complex: identification of sulfated residues and effect on ligand binding, *Biochemistry 33*, 13946−13953.
28. Michnick, D. A., Pittman, D. D., Wise, R. J., and Kaufman, R. J. (1994) Identification of individual tyrosine sulfation sites within factor VIII required for optimal activity and efficient thrombin cleavage, *J. Biol. Chem. 269*, 20095−20102.

29. Meh, D. A., Siebenlist, K. R., and Mosesson, M. W. (1996) Identification and characterization of the thrombin binding sites on fibrin, *J. Biol. Chem. 271*, 23121−23125.
30. Siebenlist, K. R., Meh, D. A., and Mosesson, M. W. (1996) Plasma factor XIII binds specifically to fibrinogen molecules containing gamma chains, *Biochemistry 35*, 10448−10453.
31. Stone, S. R., and Hofsteenge, J. (1986) Kinetics of the inhibition of thrombin by hirudin, *Biochemistry 25*, 4622−4628.
32. Trumbo, T. A., and Maurer, M. C. (2000) Examining thrombin hydrolysis of the factor XIII activation peptide segment leads to a proposal for explaining the cardioprotective effects observed with the factor XIII V34L mutation, *J. Biol. Chem. 275*, 20627−20631.
33. Winzor, D. J., and Scheraga, H. A. (1964) Titration behavior of bovine thrombin, *Arch. Biochem. Biophys. 104*, 202−207.
34. Campbell, A. P., and Sykes, B. D. (1993) The two-dimensional transferred nuclear Overhauser effect: theory and practice, *Annu. Rev. Biophys. Biomol. Struct. 22*, 99−122.
35. Ni, F. (1994) Recent developments in transferred NOE methods, *Prog. NMR Spectrosc. 26*, 517−606.
36. Trumbo, T. A., and Maurer, M. C. (2002) Thrombin hydrolysis of V29F and V34L mutants of factor XIII (28−41) reveals roles of the P(9) and P(4) positions in factor XIII activation, *Biochemistry 41*, 2859−2868.
37. Croy, C. H., Koeppe, J. R., Bergqvist, S., and Komives, E. A. (2004) Allosteric changes in solvent accessibility observed in thrombin upon active site occupation, *Biochemistry 43*, 5246−5255.
38. Mandell, J. G., Falick, A. M., and Komives, E. A. (1998) Measurement of amide hydrogen exchange by MALDI-TOF mass spectrometry, *Anal. Chem. 70*, 3987−3995.
39. Mandell, J. G., Baerga-Ortiz, A., Akashi, S., Takio, K., and Komives, E. A. (2001) Solvent accessibility of the thrombin-thrombomodulin interface, *J. Mol. Biol. 306*, 575−589.
40. Koeppe, J. R., Seitova, A., Mather, T., and Komives, E. A. (2005) Thrombomodulin tightens the thrombin active site loops to promote protein C activation, *Biochemistry 44*, 14784−14791.
41. Chen, J., and Smith, D. L. (2001) Amide hydrogen exchange shows that malate dehydrogenase is a folded monomer at pH 5, *Protein Sci. 10*, 1079−1083.
42. Wang, L., Lane, L. C., and Smith, D. L. (2001) Detecting structural changes in viral capsids by hydrogen exchange and mass spectrometry, *Protein Sci. 10*, 1234−1243.
43. Turner, B. T., Jr., and Maurer, M. C. (2002) Evaluating the roles of thrombin and calcium in the activation of coagulation factor XIII using H/D exchange and MALDI-TOF MS, *Biochemistry 41*, 7947−7954.
44. Wüthrich, K. (1986) *NMR of Proteins and Nucleic Acids*, Wiley, New York.
45. Hoofnagle, A. N., Resing, K. A., and Ahn, N. G. (2003) Protein analysis by hydrogen exchange mass spectrometry, *Annu. Rev. Biophys. Biomol. Struct. 32*, 1−25.
46. Celikel, R., McClintock, R. A., Roberts, J. R., Mendolicchio, G. L., Ware, J., Varughese, K. I., and Ruggeri, Z. M. (2003) Modulation of alpha-thrombin function by distinct interactions with platelet glycoprotein Ibalpha, *Science 301*, 218−221.
47. Dumas, J. J., Kumar, R., Seehra, J., Somers, W. S., and Mosyak, L. (2003) Crystal structure of the GpIbalpha-thrombin complex essential for platelet aggregation, *Science 301*, 222−226.
48. Hofsteenge, J., Braun, P. J., and Stone, S. R. (1988) Enzymatic properties of proteolytic derivatives of human alpha-thrombin, *Biochemistry 27*, 2144−2151.
49. Arni, R. K., Padmanabhan, K., Padmanabhan, K. P., Wu, T. P., and Tulinsky, A. (1993) Structures of the noncovalent complexes of human and bovine prothrombin fragment 2 with human PPACK-thrombin, *Biochemistry 32*, 4727−4737.
50. Carter, W. J., Cama, E., and Huntington, J. A. (2005) Crystal structure of thrombin bound to heparin, *J. Biol. Chem. 280*, 2745−2749.
51. He, X., Ye, J., Esmon, C. T., and Rezaie, A. R. (1997) Influence of Arginines 93, 97, and 101 of thrombin to its functional specificity, *Biochemistry 36*, 8969−8976.
52. Siebenlist, K. R., Mosesson, M. W., Hernandez, I., Bush, L. A., Di Cera, E., Shainoff, J. R., Di Orio, J. P., and Stojanovic, L. (2005) Studies on the basis for the properties of fibrin produced from fibrinogen-containing gamma′ chains, *Blood 106*, 2730−2736.
53. Martin, P. D., Robertson, W., Turk, D., Huber, R., Bode, W., and Edwards, B. F. (1992) The structure of residues 7−16 of the A alpha-chain of human fibrinogen bound to bovine thrombin at 2.3-Å resolution, *J. Biol. Chem. 267*, 7911−7920.
54. Fredenburgh, J. C., Stafford, A. R., and Weitz, J. I. (1997) Evidence for allosteric linkage between exosites 1 and 2 of thrombin, *J. Biol. Chem. 272*, 25493−25499.
55. Lane, D. A., Philippou, H., and Huntington, J. A. (2005) Directing thrombin, *Blood 106*, 2605−2612.
56. Verhamme, I. M., Olson, S. T., Tollefsen, D. M., and Bock, P. E. (2002) Binding of exosite ligands to human thrombin. Re-evaluation of allosteric linkage between thrombin exosites I and II, *J. Biol. Chem. 277*, 6788−6798.
57. Cristofaro, R., Carotti, A., Akhavan, S., Palla, R., Peyvandi, F., Altomare, C., and Mannucci, P. M. (2006) The natural mutation by deletion of Lys9 in the thrombin A-chain affects the p*K* value of catalytic residues, the overall enzyme's stability and conformational transitions linked to Na binding, *FEBS J. 273*, 159−169.

BI060360K